

Precise measurement of the χ_{c0} resonance parameters and branching fractions of $\chi_{c0,c2} \rightarrow \pi^+ \pi^- / K^+ K^-$ *

M. Ablikim (麦迪娜)¹ M. N. Achasov^{4,c} P. Adlarson⁷⁶ O. Afedulidis³ X. C. Ai (艾小聪)⁸¹ R. Aliberti³⁵
 A. Amoroso^{75A,75C} Y. Bai (白羽)⁵⁷ O. Bakina³⁶ I. Balossino^{29A} Y. Ban (班勇)^{46,h} H.-R. Bao (包浩然)⁶⁴
 V. Batozskaya^{1,44} K. Begzsuren³² N. Berger³⁵ M. Berlowski⁴⁴ M. Bertani^{28A} D. Bettoni^{29A} F. Bianchi^{75A,75C}
 E. Bianco^{75A,75C} A. Bortone^{75A,75C} I. Boyko³⁶ R. A. Briere⁵ A. Brueggemann⁶⁹ H. Cai (蔡浩)⁷⁷ X. Cai (蔡啸)^{1,58}
 A. Calcaterra^{28A} G. F. Cao (曹国富)^{1,64} N. Cao (曹宁)^{1,64} S. A. Cetin^{62A} X. Y. Chai (柴新宇)^{46,h}
 J. F. Chang (常劲帆)^{1,58} G. R. Che (车国荣)⁴³ Y. Z. Che (车逾之)^{1,58,64} G. Chelkov^{36,b} C. Chen (陈琛)⁴³
 C. H. Chen (陈春卉)⁹ Chao Chen (陈超)⁵⁵ G. Chen (陈刚)¹ H. S. Chen (陈和生)^{1,64} H. Y. Chen (陈弘扬)²⁰
 M. L. Chen (陈玛丽)^{1,58,64} S. J. Chen (陈申见)⁴² S. L. Chen (陈思璐)⁴⁵ S. M. Chen (陈少敏)⁶¹ T. Chen (陈通)^{1,64}
 X. R. Chen (陈旭荣)^{31,64} X. T. Chen (陈肖婷)^{1,64} Y. B. Chen (陈元柏)^{1,58} Y. Q. Chen³⁴ Z. J. Chen^{25,i}
 Z. Y. Chen (陈正元)^{1,64} S. K. Choi¹⁰ G. Cibinetto^{29A} F. Cossio^{75C} J. J. Cui⁵⁰ H. L. Dai^{1,58} J. P. Dai (代建平)⁷⁹
 A. Dbeysi¹⁸ R. E. de Boer³ D. Dedovich³⁶ C. Q. Deng (邓创旗)⁷³ Z. Y. Deng (邓子艳)¹ A. Denig³⁵
 I. Denisenko³⁶ M. Destefanis^{75A,75C} F. De Mori^{75A,75C} B. Ding (丁彪)^{67,1} X. X. Ding (丁晓萱)^{46,h} Y. Ding (丁勇)⁴⁰
 Y. Ding³⁴ J. Dong (董静)^{1,58} L. Y. Dong (董燎原)^{1,64} M. Y. Dong (董明义)^{1,58,64} X. Dong (董翔)⁷⁷
 M. C. Du (杜蒙川)¹ S. X. Du (杜书先)⁸¹ Y. Y. Duan (段尧予)⁵⁵ Z. H. Duan (段宗欢)⁴² P. Egorov^{36,b}
 Y. H. Fan (范宇晗)⁴⁵ J. Fang (方建)^{1,58} J. Fang (方进)⁵⁹ S. S. Fang (房双世)^{1,64} W. X. Fang (方文兴)¹
 Y. Fang (方易)¹ Y. Q. Fang (方亚泉)^{1,58} R. Farinelli^{29A} L. Fava^{75B,75C} F. Feldbauer³ G. Felici^{28A}
 C. Q. Feng (封常青)^{72,58} J. H. Feng⁵⁹ Y. T. Feng (冯琦潼)^{72,58} M. Fritsch³ C. D. Fu (傅成栋)¹ J. L. Fu (傅金林)⁶⁴
 Y. W. Fu (傅亦威)^{1,64} H. Gao (高涵)⁶⁴ X. B. Gao (高鑫博)⁴¹ Y. N. Gao^{46,h} Yang Gao (高扬)^{72,58} S. Garbolino^{75C}
 I. Garzia^{29A,29B} L. Ge⁸¹ P. T. Ge (葛潘婷)¹⁹ Z. W. Ge (葛振武)⁴² C. Geng (耿聪)⁵⁹ E. M. Gersabeck⁶⁸ A. Gilman⁷⁰
 K. Goetzen¹³ L. Gong (龚丽)⁴⁰ W. X. Gong (龚文焯)^{1,58} W. Gradl³⁵ S. Gramigna^{29A,29B} M. Greco^{75A,75C}
 M. H. Gu (顾昱皓)^{1,58} Y. T. Gu (顾运厅)¹⁵ C. Y. Guan (关春懿)^{1,64} A. Q. Guo (郭爱强)^{31,64} L. B. Guo (郭立波)⁴¹
 M. J. Guo (国梦娇)⁵⁰ R. P. Guo (郭如盼)⁴⁹ Y. P. Guo (郭玉萍)^{12,g} A. Guskov^{36,b} J. Gutierrez²⁷
 K. L. Han (韩坤霖)⁶⁴ T. T. Han (韩婷婷)¹ F. Hanisch³ X. Q. Hao (郝喜庆)¹⁹ F. A. Harris⁶⁶ K. K. He (何凯凯)⁵⁵
 K. L. He (何康林)^{1,64} F. H. Heinsius³ C. H. Heinz³⁵ Y. K. Heng (衡月昆)^{1,58,64} C. Herold⁶⁰ T. Holtmann³
 P. C. Hong (洪鹏程)³⁴ G. Y. Hou (侯国一)^{1,64} X. T. Hou (侯贤涛)^{1,64} Y. R. Hou (侯颖锐)⁶⁴ Z. L. Hou (侯治龙)¹
 B. Y. Hu⁵⁹ H. M. Hu (胡海明)^{1,64} J. F. Hu (胡继峰)^{56,j} Q. P. Hu (胡启鹏)^{72,58} S. L. Hu (胡圣亮)^{12,g}
 T. Hu (胡涛)^{1,58,64} Y. Hu (胡誉)¹ G. S. Huang (黄光顺)^{72,58} K. X. Huang (黄凯旋)⁵⁹ L. Q. Huang (黄麟钦)^{31,64}
 X. T. Huang (黄性涛)⁵⁰ Y. P. Huang (黄燕萍)¹ Y. S. Huang (黄永盛)⁵⁹ T. Hussain⁷⁴ F. Hölzken³ N. Hüskens³⁵
 N. in der Wiesche⁶⁹ J. Jackson²⁷ S. Janchiv³² J. H. Jeong¹⁰ Q. Ji (纪全)¹ Q. P. Ji (姬清平)¹⁹ W. Ji (季旺)^{1,64}

Received 27 June 2025; Accepted 30 June 2025; Published online 1 July 2025

* Supported in part by National Key R&D Program of China (2020YFA0406300, 2020YFA0406400, 2023YFA1606000); National Natural Science Foundation of China (NSFC) (11635010, 11735014, 11935015, 11935016, 11935018, 12025502, 12035009, 12035013, 12061131003, 12192260, 12192261, 12192262, 12192263, 12192264, 12192265, 12221005, 12225509, 12235017, 12361141819); the Chinese Academy of Sciences (CAS) Large-Scale Scientific Facility Program; the CAS Center for Excellence in Particle Physics (CCEPP); Joint Large-Scale Scientific Facility Funds of the NSFC and CAS (U1832207); 100 Talents Program of CAS; (ZR2022JQ02, ZR2024QA151) supported by Shandong Provincial Natural Science Foundation; supported by the China Postdoctoral Science Foundation (2023M742100); The Institute of Nuclear and Particle Physics (INPAC) and Shanghai Key Laboratory for Particle Physics and Cosmology; German Research Foundation DFG (FOR5327, GRK 2149); Istituto Nazionale di Fisica Nucleare, Italy; Knut and Alice Wallenberg Foundation (2021.0174, 2021.0299); Ministry of Development of Turkey (DPT2006K-120470); National Research Foundation of Korea (NRF-2022R1A2C1092335); National Science and Technology fund of Mongolia; National Science Research and Innovation Fund (NSRF) via the Program Management Unit for Human Resources & Institutional Development, Research and Innovation of Thailand (B16F640076, B50G670107); Polish National Science Centre (2019/35/O/ST2/02907); Swedish Research Council (2019.04595); The Swedish Foundation for International Cooperation in Research and Higher Education (CH2018-7756); U. S. Department of Energy (DE-FG02-05ER41374)



Content from this work may be used under the terms of the Creative Commons Attribution 3.0 licence. Any further distribution of this work must maintain attribution to the author(s) and the title of the work, journal citation and DOI. Article funded by SCOAP³ and published under licence by Chinese Physical Society and the Institute of High Energy Physics of the Chinese Academy of Sciences and the Institute of Modern Physics of the Chinese Academy of Sciences and IOP Publishing Ltd

- X. B. Ji (季晓斌)^{1,64} X. L. Ji (季筱璐)^{1,58} Y. Y. Ji⁵⁰ X. Q. Jia (贾晓倩)⁵⁰ Z. K. Jia (贾泽坤)^{72,58} D. Jiang (姜地)^{1,64}
H. B. Jiang (姜候兵)⁷⁷ P. C. Jiang (蒋沛成)^{46,h} S. S. Jiang (姜赛赛)³⁹ T. J. Jiang¹⁶ X. S. Jiang (江晓山)^{1,58,64}
Y. Jiang (蒋艺)⁶⁴ J. B. Jiao (焦健斌)⁵⁰ J. K. Jiao (焦俊坤)³⁴ Z. Jiao (焦铮)²³ S. Jin (金山)⁴² Y. Jin (金毅)⁶⁷
M. Q. Jing (荆茂强)^{1,64} X. M. Jing (景新媚)⁶⁴ T. Johansson⁷⁶ S. Kabana³³ N. Kalantar-Nayestanaki⁶⁵
X. L. Kang (康晓琳)⁹ X. S. Kang (康晓坤)⁴⁰ M. Kavatsyuk⁶⁵ B. C. Ke (柯百谦)⁸¹ V. Khachatryan²⁷ A. Khoukaz⁶⁹
R. Kiuchi¹ O. B. Kolcu^{62A} B. Kopf³ M. Kuessner³ X. Kui (奎贤)^{1,64} N. Kumar²⁶ A. Kupsc^{44,76} W. Kühn³⁷
L. Lavezzi^{75A,75C} T. T. Lei (雷天天)^{72,58} Z. H. Lei^{72,58} M. Lellmann³⁵ T. Lenz³⁵ C. Li⁴³ C. Li (李翠)⁴⁷
C. H. Li (李春花)³⁹ Cheng Li^{72,58} D. M. Li (李德民)⁸¹ F. Li (李飞)^{1,58} G. Li (李刚)¹ H. B. Li (李海波)^{1,64}
H. J. Li (李惠静)¹⁹ H. N. Li (李衡讷)^{56,j} Hui Li (李慧)⁴³ J. R. Li (李嘉荣)⁶¹ J. S. Li (李静舒)⁵⁹ K. Li (李科)¹
K. L. Li (李凯璐)¹⁹ L. J. Li (李林健)^{1,64} L. K. Li (李龙科)¹ Lei Li (李蕾)⁴⁸ M. H. Li (李明浩)⁴³
P. R. Li (李培荣)^{38,k,1} Q. M. Li (李启铭)^{1,64} Q. X. Li (李起鑫)⁵⁰ R. Li (李燃)^{17,31} S. X. Li (李素娴)¹² T. Li (李腾)⁵⁰
T. Y. Li (李天佑)⁴³ W. D. Li (李卫东)^{1,64} W. G. Li (李卫国)^{1,a} X. Li (李旭)^{1,64} X. H. Li (李旭红)^{72,58}
X. L. Li (李晓玲)⁵⁰ X. Y. Li (李晓宇)^{1,8} X. Z. Li (李绪泽)⁵⁹ Y. G. Li (李彦谷)^{46,h} Z. J. Li (李志军)⁵⁹
Z. Y. Li (李紫阳)⁷⁹ C. Liang (梁畅)⁴² H. Liang (梁昊)^{72,58} H. Liang^{1,64} Y. F. Liang (梁勇飞)⁵⁴
Y. T. Liang (梁羽铁)^{31,64} G. R. Liao (廖广睿)¹⁴ Y. P. Liao (廖一朴)^{1,64} J. Libby²⁶ A. Limphirat⁶⁰
C. C. Lin (蔺长城)⁵⁵ C. X. Lin (林创新)⁶⁴ D. X. Lin (林德旭)^{31,64} T. Lin (林韬)¹ B. J. Liu (刘北江)¹
B. X. Liu (刘宝鑫)⁷⁷ C. Liu (刘成)³⁴ C. X. Liu (刘春秀)¹ F. Liu (刘芳)¹ F. H. Liu (刘福虎)⁵³ Feng Liu (刘峰)⁶
G. M. Liu (刘国明)^{56,j} H. Liu (刘昊)^{38,k,1} H. B. Liu (刘宏邦)¹⁵ H. H. Liu (刘欢欢)¹ H. M. Liu (刘怀民)^{1,64}
Huihui Liu (刘汇慧)²¹ J. B. Liu (刘建北)^{72,58} J. Y. Liu (刘晶译)^{1,64} K. Liu (刘凯)^{38,k,1} K. Y. Liu (刘魁勇)⁴⁰
Ke Liu (刘珂)²² L. Liu^{72,58} L. C. Liu (刘良辰)⁴³ Lu Liu (刘露)⁴³ M. H. Liu (刘美宏)^{12,g} P. L. Liu (刘佩莲)¹
Q. Liu (刘倩)⁶⁴ S. B. Liu (刘树彬)^{72,58} T. Liu (刘桐)^{12,g} W. K. Liu (刘维克)⁴³ W. M. Liu (刘卫民)^{72,58}
X. Liu (刘翔)^{38,k,1} X. Liu (刘鑫)³⁹ Y. Liu⁸¹ Y. Liu (刘英)^{38,k,1} Y. B. Liu (刘玉斌)⁴³ Z. A. Liu (刘振安)^{1,58,64}
Z. D. Liu (刘宗德)⁹ Z. Q. Liu (刘智青)⁵⁰ X. C. Lou (娄辛丑)^{1,58,64} F. X. Lu⁵⁹ H. J. Lu (吕海江)²³
J. G. Lu (吕军光)^{1,58} X. L. Lu (陆小玲)¹ Y. Lu (卢宇)⁷ Y. P. Lu (卢云鹏)^{1,58} Z. H. Lu (卢泽辉)^{1,64}
C. L. Luo (罗成林)⁴¹ J. R. Luo (罗家瑞)⁵⁹ M. X. Luo (罗民兴)⁸⁰ T. Luo (罗涛)^{12,g} X. L. Luo (罗小兰)^{1,58}
X. R. Lyu (吕晓睿)⁶⁴ Y. F. Lyu (吕翌丰)⁴³ F. C. Ma (马凤才)⁴⁰ H. Ma (马衡)⁷⁹ H. L. Ma (马海龙)¹
J. L. Ma (马俊力)^{1,64} L. L. Ma (马连良)⁵⁰ L. R. Ma (马立瑞)⁶⁷ M. M. Ma (马明明)^{1,64} Q. M. Ma (马秋梅)¹
R. Q. Ma (马润秋)^{1,64} T. Ma (马腾)^{72,58} X. T. Ma (马晓天)^{1,64} X. Y. Ma (马骁妍)^{1,58} Y. M. Ma (马玉明)³¹
F. E. Maas¹⁸ I. MacKay⁷⁰ M. Maggiora^{75A,75C} S. Malde⁷⁰ Y. J. Mao (冒亚军)^{46,h} Z. P. Mao (毛泽普)¹
S. Marcello^{75A,75C} Z. X. Meng (孟召霞)⁶⁷ J. G. Messchendorp^{13,65} G. Mezzadri^{29A} H. Miao (妙哈)^{1,64}
T. J. Min (闵天觉)⁴² R. E. Mitchell²⁷ X. H. Mo (莫晓虎)^{1,58,64} B. Moses²⁷ N. Yu. Muchnoi^{4,c} J. Muskalla³⁵
Y. Nefedov³⁶ F. Nerling^{18,e} L. S. Nie²⁰ I. B. Nikolaev^{4,c} Z. Ning (宁哲)^{1,58} S. Nisar^{11,m} Q. L. Niu (牛祺乐)^{38,k,1}
W. D. Niu (牛文迪)⁵⁵ Y. Niu (牛艳)⁵⁰ S. L. Olsen⁶⁴ S. L. Olsen^{10,64} Q. Ouyang (欧阳群)^{1,58,64} S. Pacetti^{28B,28C}
X. Pan (潘祥)⁵⁵ Y. Pan (潘越)⁵⁷ A. Pathak³⁴ Y. P. Pei (裴宇鹏)^{72,58} M. Pelizaeus³ H. P. Peng (彭海平)^{72,58}
Y. Y. Peng (彭云翊)^{38,k,1} K. Peters^{13,e} J. L. Ping (平加伦)⁴¹ R. G. Ping (平荣刚)^{1,64} S. Plura³⁵ V. Prasad³³
F. Z. Qi (齐法制)¹ H. Qi^{72,58} H. R. Qi (漆红荣)⁶¹ M. Qi (祁鸣)⁴² T. Y. Qi (齐天钰)^{12,g} S. Qian (钱森)^{1,58}
W. B. Qian (钱文斌)⁶⁴ C. F. Qiao (乔从丰)⁶⁴ X. K. Qiao⁸¹ J. J. Qin (秦佳佳)⁷³ L. Q. Qin (秦丽清)¹⁴
L. Y. Qin (秦龙宇)^{72,58} X. P. Qin (覃潇平)^{12,g} X. S. Qin (秦小帅)⁵⁰ Z. H. Qin (秦中华)^{1,58} J. F. Qiu (邱进发)¹
Z. H. Qu (屈子皓)⁷³ C. F. Redmer³⁵ K. J. Ren (任旷洁)³⁹ A. Rivetti^{75C} M. Rolo^{75C} G. Rong (荣刚)^{1,64}
Ch. Rosner¹⁸ M. Q. Ruan (阮曼奇)^{1,58} S. N. Ruan (阮氏宁)⁴³ N. Salone⁴⁴ A. Sarantsev^{36,d} Y. Schelhaas³⁵
K. Schoenning⁷⁶ M. Scodreggio^{29A} K. Y. Shan (尚科羽)^{12,g} W. Shan (单葳)²⁴ X. Y. Shan (单心钰)^{72,58}
Z. J. Shang (尚子杰)^{38,k,1} J. F. Shanguan (上官剑锋)¹⁶ L. G. Shao (邵立港)^{1,64} M. Shao (邵明)^{72,58}
C. P. Shen (沈成平)^{12,g} H. F. Shen (沈宏飞)^{1,8} W. H. Shen (沈文涵)⁶⁴ X. Y. Shen (沈肖雁)^{1,64} B. A. Shi (施伯安)⁶⁴
H. Shi (史华)^{72,58} J. L. Shi (石家磊)^{12,g} J. Y. Shi (石京燕)¹ Q. Q. Shi (石勤强)⁵⁵ S. Y. Shi (史书宇)⁷³
X. Shi (史欣)^{1,58} J. J. Song (宋娇娇)¹⁹ T. Z. Song (宋天资)⁵⁹ W. M. Song (宋维民)^{34,1} Y. J. Song (宋宇镜)^{12,g}
Y. X. Song (宋昀轩)^{46,h,n} S. Sosio^{75A,75C} S. Spataro^{75A,75C} F. Stielor³⁵ S. S. Su (苏闪闪)⁴⁰ Y. J. Su (粟捷扬)⁶⁴

- G. B. Sun (孙光豹)⁷⁷ G. X. Sun (孙功星)¹ H. Sun (孙昊)⁶⁴ H. K. Sun (孙浩凯)¹ J. F. Sun (孙俊峰)¹⁹
 K. Sun (孙开)⁶¹ L. Sun (孙亮)⁷⁷ S. S. Sun (孙胜森)^{1,64} T. Sun^{51,f} W. Y. Sun (孙文玉)³⁴ Y. Sun (孙源)⁹
 Y. J. Sun (孙勇杰)^{72,58} Y. Z. Sun (孙永昭)¹ Z. Q. Sun (孙泽群)^{1,64} Z. T. Sun (孙振田)⁵⁰ C. J. Tang (唐昌建)⁵⁴
 G. Y. Tang (唐光毅)¹ J. Tang (唐健)⁵⁹ J. J. Tang (唐嘉骏)^{72,58} Y. A. Tang (唐迎澳)⁷⁷ L. Y. Tao (陶璐燕)⁷³
 Q. T. Tao (陶秋田)^{25,i} M. Tat⁷⁰ J. X. Teng (滕佳秀)^{72,58} V. Thoren⁷⁶ W. H. Tian (田文辉)⁵⁹ Y. Tian (田野)^{31,64}
 Z. F. Tian (田喆飞)⁷⁷ I. Uman^{62B} Y. Wan (万宇)⁵⁵ S. J. Wang⁵⁰ B. Wang (王斌)¹ B. L. Wang (王滨龙)⁶⁴
 Bo Wang (王博)^{72,58} D. Y. Wang (王大勇)^{46,h} F. Wang (王菲)⁷³ H. J. Wang (王泓鉴)^{38,k,1} J. J. Wang (王家驹)⁷⁷
 J. P. Wang (王吉鹏)⁵⁰ K. Wang (王科)^{1,58} L. L. Wang (王亮亮)¹ M. Wang (王萌)⁵⁰ N. Y. Wang (王南洋)⁶⁴
 S. Wang (王顺)^{12,g} S. Wang^{38,k,1} T. Wang (王婷)^{12,g} T. J. Wang (王腾蛟)⁴³ W. Wang⁵⁹ W. Wang (王维)⁷³
 W. P. Wang (王维平)^{35,58,72,o} X. Wang (王轩)^{46,h} X. F. Wang (王雄飞)^{38,k,1} X. J. Wang (王希俊)³⁹
 X. L. Wang (王小龙)^{12,g} X. N. Wang (王新南)^{1,64} Y. Wang (王亦)⁶¹ Y. D. Wang (王雅迪)⁴⁵
 Y. F. Wang (王贻芳)^{1,58,64} Y. H. Wang (王英豪)^{38,k,1} Y. L. Wang (王艺龙)¹⁹ Y. N. Wang (王亚男)⁴⁵
 Y. Q. Wang (王雨晴)¹ Yaqian Wang (王亚乾)¹⁷ Yi Wang (王义)⁶¹ Z. Wang (王铮)^{1,58} Z. L. Wang (王治浪)⁷³
 Z. Y. Wang (王至勇)^{1,64} Ziyi Wang (王子一)⁶⁴ D. H. Wei (魏代会)¹⁴ F. Weidner⁶⁹ S. P. Wen (文硕频)¹
 Y. R. Wen (温亚冉)³⁹ U. Wiedner³ G. Wilkinson⁷⁰ M. Wolke⁷⁶ L. Wollenberg³ C. Wu (吴晨)³⁹
 J. F. Wu (吴金飞)^{1,8} L. H. Wu (伍灵慧)¹ L. J. Wu (吴连近)^{1,64} X. Wu (吴潇)^{12,g} X. H. Wu (伍雄浩)³⁴ Y. Wu^{72,58}
 Y. H. Wu (吴业昊)⁵⁵ Y. J. Wu (吴英杰)³¹ Z. Wu (吴智)^{1,58} L. Xia (夏磊)^{72,58} X. M. Xian (咸秀梅)³⁹
 B. H. Xiang (向本后)^{1,64} T. Xiang^{46,h} D. Xiao (肖栋)^{38,k,1} G. Y. Xiao (肖光延)⁴² S. Y. Xiao (肖素玉)¹
 Y. L. Xiao (肖云龙)^{12,g} Z. J. Xiao (肖振军)⁴¹ C. Xie (谢陈)⁴² X. H. Xie^{46,h} Y. Xie (谢勇)⁵⁰ Y. G. Xie (谢宇广)^{1,58}
 Y. H. Xie (谢跃红)⁶ Z. P. Xie (谢智鹏)^{72,58} T. Y. Xing (邢天宇)^{1,64} C. F. Xu^{1,64} C. J. Xu (许创杰)⁵⁹
 G. F. Xu (许国发)¹ H. Y. Xu (许皓月)^{67,2} M. Xu (徐明)^{72,58} Q. J. Xu (徐庆君)¹⁶ Q. N. Xu³⁰ W. Xu (许威)¹
 W. L. Xu (徐万伦)⁶⁷ X. P. Xu (徐新平)⁵⁵ Y. Xu (徐月)⁴⁰ Y. C. Xu (胥英超)⁷⁸ Z. S. Xu (许昭燊)⁶⁴
 F. Yan (严芳)^{12,g} L. Yan (严亮)^{12,g} W. B. Yan (鄢文标)^{72,58} W. C. Yan (闫文成)⁸¹ X. Q. Yan (严薛强)^{1,64}
 H. J. Yang (杨海军)^{51,f} H. L. Yang (杨昊霖)³⁴ H. X. Yang (杨洪勋)¹ J. H. Yang (杨君辉)⁴² T. Yang¹
 Y. Yang (杨莹)^{12,g} Y. F. Yang (杨翊凡)^{1,64} Y. F. Yang (杨艳芳)⁴³ Y. X. Yang (杨逸翔)^{1,64} Z. W. Yang (杨政武)^{38,k,1}
 Z. P. Yao (姚志鹏)⁵⁰ M. Ye (叶梅)^{1,58} M. H. Ye (叶铭汉)⁸ J. H. Yin (殷俊昊)¹ Junhao Yin (殷俊昊)⁴³
 Z. Y. You (尤邦昀)⁵⁹ B. X. Yu (俞伯祥)^{1,58,64} C. X. Yu (喻纯旭)⁴³ G. Yu (余刚)^{1,64} J. S. Yu (俞洁晟)^{25,i} M. C. Yu⁴⁰
 T. Yu (于涛)⁷³ X. D. Yu (余旭东)^{46,h} Y. C. Yu⁸¹ C. Z. Yuan (苑长征)^{1,64} J. Yuan⁴⁵ J. Yuan (袁菁)³⁴
 L. Yuan (袁丽)² S. C. Yuan (苑思成)^{1,64} Y. Yuan (袁野)^{1,64} Z. Y. Yuan (袁朝阳)⁵⁹ C. X. Yue (岳崇兴)³⁹
 A. A. Zafar⁷⁴ F. R. Zeng (曾凡蕊)⁵⁰ S. H. Zeng⁶³ X. Zeng (曾鑫)^{12,g} Y. Zeng^{25,i} Y. J. Zeng (曾溢嘉)^{1,64} Y.
 J. Zeng (曾宇杰)⁵⁹ X. Y. Zhai (翟星晔)³⁴ Y. C. Zhai (翟云聪)⁵⁰ Y. H. Zhan (詹永华)⁵⁹ A. Q. Zhang (张安庆)^{1,64} B.
 L. Zhang (张伯伦)^{1,64} B. X. Zhang (张丙新)¹ D. H. Zhang (张丹昊)⁴³ G. Y. Zhang (张广义)¹⁹
 H. Zhang (张哈)⁸¹ H. Zhang (张豪)^{72,58} H. C. Zhang (张航畅)^{1,58,64} H. H. Zhang³⁴ H. H. Zhang (张宏浩)⁵⁹
 H. Q. Zhang (张华桥)^{1,58,64} H. R. Zhang (张浩然)^{72,58} H. Y. Zhang (章红宇)^{1,58} J. Zhang⁸¹ J. Zhang (张晋)⁵⁹
 J. J. Zhang (张进军)⁵² J. L. Zhang (张杰磊)²⁰ J. Q. Zhang (张敬庆)⁴¹ J. S. Zhang (张家声)^{12,g}
 J. W. Zhang (张家文)^{1,58,64} J. X. Zhang (张景旭)^{38,k,1} J. Y. Zhang (张建勇)¹ J. Z. Zhang (张景芝)^{1,64}
 Jianyu Zhang (张剑宇)⁶⁴ L. M. Zhang (张黎明)⁶¹ Lei Zhang (张雷)⁴² P. Zhang (张鹏)^{1,64} Q. Y. Zhang (张秋岩)³⁴
 R. Y. Zhang (张若愚)^{38,k,1} S. H. Zhang (张水涵)^{1,64} Shulei Zhang (张书磊)^{25,i} X. M. Zhang (张晓梅)¹ X. Y. Zhang⁴⁰
 X. Y. Zhang (张学尧)⁵⁰ Y. Zhang (张瑶)¹ Y. Zhang (张宇)⁷³ Y. T. Zhang (张亚腾)⁸¹ Y. H. Zhang (张银鸿)^{1,58}
 Y. M. Zhang (张悦明)³⁹ Yan Zhang^{72,58} Z. D. Zhang (张正德)¹ Z. H. Zhang (张泽恒)¹ Z. L. Zhang (张兆领)³⁴
 Z. Y. Zhang (张子羽)⁴³ Z. Y. Zhang (张振宇)⁷⁷ Z. Z. Zhang (张子扬)⁴⁵ G. Zhao (赵光)¹ J. Y. Zhao (赵静宜)^{1,64}
 J. Z. Zhao (赵京周)^{1,58} L. Zhao¹ L. Zhao (赵雷)^{72,58} M. G. Zhao (赵明刚)⁴³ N. Zhao (赵宁)⁷⁹ R. P. Zhao (赵若平)⁶⁴
 S. J. Zhao (赵书俊)⁸¹ Y. B. Zhao (赵豫斌)^{1,58} Y. X. Zhao (赵宇翔)^{31,64} Z. G. Zhao (赵政国)^{72,58} A. Zhemchugov^{36,b}
 B. Zheng (郑波)⁷³ B. M. Zheng (郑变敏)³⁴ J. P. Zheng (郑建平)^{1,58} W. J. Zheng (郑文静)^{1,64}
 Y. H. Zheng (郑阳恒)⁶⁴ B. Zhong (钟彬)⁴¹ X. Zhong⁵⁹ H. Zhou (周航)⁵⁰ J. Y. Zhou (周佳莹)³⁴
 L. P. Zhou (周利鹏)^{1,64} S. Zhou (周帅)⁶ X. Zhou (周详)⁷⁷ X. K. Zhou (周晓康)⁶ X. R. Zhou (周小蓉)^{72,58}

X. Y. Zhou (周兴玉)³⁹ Y. Z. Zhou (周祎卓)^{12,g} Z. C. Zhou²⁰ A. N. Zhu (朱傲男)⁶⁴ J. Zhu (朱江)⁴³ K. Zhu (朱凯)¹
 K. J. Zhu (朱科军)^{1,58,64} K. S. Zhu (朱康帅)^{12,g} L. Zhu (朱林)³⁴ L. X. Zhu (朱琳萱)⁶⁴ S. H. Zhu (朱世海)⁷¹
 T. J. Zhu (朱腾蛟)^{12,g} W. D. Zhu (朱稳定)⁴¹ Y. C. Zhu (朱莹春)^{72,58} Z. A. Zhu (朱自安)^{1,64}
 J. H. Zou (邹佳恒)¹ J. Zu (祖健)^{72,58}

(BESIII Collaboration)

- ¹Institute of High Energy Physics, Beijing 100049, China
²Beihang University, Beijing 100191, China
³Bochum Ruhr-University, D-44780 Bochum, Germany
⁴Budker Institute of Nuclear Physics SB RAS (BINP), Novosibirsk 630090, Russia
⁵Carnegie Mellon University, Pittsburgh, Pennsylvania 15213, USA
⁶Central China Normal University, Wuhan 430079, China
⁷Central South University, Changsha 410083, China
⁸China Center of Advanced Science and Technology, Beijing 100190, China
⁹China University of Geosciences, Wuhan 430074, China
¹⁰Chung-Ang University, Seoul, 06974, Republic of Korea
¹¹COMSATS University Islamabad, Lahore Campus, Defence Road, Off Raiwind Road, 54000 Lahore, Pakistan
¹²Fudan University, Shanghai 200433, China
¹³GSI Helmholtzcentre for Heavy Ion Research GmbH, D-64291 Darmstadt, Germany
¹⁴Guangxi Normal University, Guilin 541004, China
¹⁵Guangxi University, Nanning 530004, China
¹⁶Hangzhou Normal University, Hangzhou 310036, China
¹⁷Hebei University, Baoding 071002, China
¹⁸Helmholtz Institute Mainz, Staudinger Weg 18, D-55099 Mainz, Germany
¹⁹Henan Normal University, Xinxiang 453007, China
²⁰Henan University, Kaifeng 475004, China
²¹Henan University of Science and Technology, Luoyang 471003, China
²²Henan University of Technology, Zhengzhou 450001, China
²³Huangshan College, Huangshan 245000, China
²⁴Hunan Normal University, Changsha 410081, China
²⁵Hunan University, Changsha 410082, China
²⁶Indian Institute of Technology Madras, Chennai 600036, India
²⁷Indiana University, Bloomington, Indiana 47405, USA
^{28A}INFN Laboratori Nazionali di Frascati, I-00044, Frascati, Italy
^{28B}INFN Laboratori Nazionali di Frascati, INFN Sezione di Perugia, I-06100, Perugia, Italy
^{28C}INFN Laboratori Nazionali di Frascati, University of Perugia, I-06100, Perugia, Italy
^{29A}INFN Sezione di Ferrara, I-44122, Ferrara, Italy
^{29B}INFN Sezione di Ferrara, University of Ferrara, I-44122, Ferrara, Italy
³⁰Inner Mongolia University, Hohhot 010021, China
³¹Institute of Modern Physics, Lanzhou 730000, China
³²Institute of Physics and Technology, Peace Avenue 54B, Ulaanbaatar 13330, Mongolia
³³Instituto de Alta Investigación, Universidad de Tarapacá, Casilla 7D, Arica 1000000, Chile
³⁴Jilin University, Changchun 130012, China
³⁵Johannes Gutenberg University of Mainz, Johann-Joachim-Becher-Weg 45, D-55099 Mainz, Germany
³⁶Joint Institute for Nuclear Research, 141980 Dubna, Moscow region, Russia
³⁷Justus-Liebig-Universität Giessen, II. Physikalisches Institut, Heinrich-Buff-Ring 16, D-35392 Giessen, Germany
³⁸Lanzhou University, Lanzhou 730000, China
³⁹Liaoning Normal University, Dalian 116029, China
⁴⁰Liaoning University, Shenyang 110036, China
⁴¹Nanjing Normal University, Nanjing 210023, China
⁴²Nanjing University, Nanjing 210093, China
⁴³Nankai University, Tianjin 300071, China
⁴⁴National Centre for Nuclear Research, Warsaw 02-093, Poland
⁴⁵North China Electric Power University, Beijing 102206, China
⁴⁶Peking University, Beijing 100871, China
⁴⁷Qufu Normal University, Qufu 273165, China
⁴⁸Renmin University of China, Beijing 100872, China
⁴⁹Shandong Normal University, Jinan 250014, China
⁵⁰Shandong University, Jinan 250100, China
⁵¹Shanghai Jiao Tong University, Shanghai 200240, China
⁵²Shanxi Normal University, Linfen 041004, China
⁵³Shanxi University, Taiyuan 030006, China
⁵⁴Sichuan University, Chengdu 610064, China
⁵⁵Soochow University, Suzhou 215006, China
⁵⁶South China Normal University, Guangzhou 510006, China
⁵⁷Southeast University, Nanjing 211100, China
⁵⁸State Key Laboratory of Particle Detection and Electronics, Beijing 100049, Hefei 230026, China

⁵⁹Sun Yat-Sen University, Guangzhou 510275, China⁶⁰Suranaree University of Technology, University Avenue 111, Nakhon Ratchasima 30000, Thailand⁶¹Tsinghua University, Beijing 100084, China^{62A}Turkish Accelerator Center Particle Factory Group, Istinye University, 34010, Istanbul, Turkey^{62B}Turkish Accelerator Center Particle Factory Group, Near East University, Nicosia, North Cyprus, 99138, Mersin 10, Turkey⁶³University of Bristol, H H Wills Physics Laboratory, Tyndall Avenue, Bristol, BS8 1TL, UK⁶⁴University of Chinese Academy of Sciences, Beijing 100049, China⁶⁵University of Groningen, NL-9747 AA Groningen, The Netherlands⁶⁶University of Hawaii, Honolulu, Hawaii 96822, USA⁶⁷University of Jinan, Jinan 250022, China⁶⁸University of Manchester, Oxford Road, Manchester, M13 9PL, United Kingdom⁶⁹University of Muenster, Wilhelm-Klemm-Strasse 9, 48149 Muenster, Germany⁷⁰University of Oxford, Keble Road, Oxford OX13RH, United Kingdom⁷¹University of Science and Technology Liaoning, Anshan 114051, China⁷²University of Science and Technology of China, Hefei 230026, China⁷³University of South China, Hengyang 421001, China⁷⁴University of the Punjab, Lahore-54590, Pakistan^{75A}University of Turin and INFN, University of Turin, I-10125, Turin, Italy^{75B}University of Turin and INFN, University of Eastern Piedmont, I-15121, Alessandria, Italy^{75C}University of Turin and INFN, INFN, I-10125, Turin, Italy⁷⁶Uppsala University, Box 516, SE-75120 Uppsala, Sweden⁷⁷Wuhan University, Wuhan 430072, China⁷⁸Yantai University, Yantai 264005, China⁷⁹Yunnan University, Kunming 650500, China⁸⁰Zhejiang University, Hangzhou 310027, China⁸¹Zhengzhou University, Zhengzhou 450001, China^aDeceased^bAlso at the Moscow Institute of Physics and Technology, Moscow 141700, Russia^cAlso at the Novosibirsk State University, Novosibirsk, 630090, Russia^dAlso at the NRC "Kurchatov Institute", PNPI, 188300, Gatchina, Russia^eAlso at Goethe University Frankfurt, 60323 Frankfurt am Main, Germany^fAlso at Key Laboratory for Particle Physics, Astrophysics and Cosmology, Ministry of Education; Shanghai Key Laboratory for Particle Physics and Cosmology; Institute of Nuclear and Particle Physics, Shanghai 200240, China^gAlso at Key Laboratory of Nuclear Physics and Ion-beam Application (MOE) and Institute of Modern Physics, Fudan University, Shanghai 200443, China^hAlso at State Key Laboratory of Nuclear Physics and Technology, Peking University, Beijing 100871, ChinaⁱAlso at School of Physics and Electronics, Hunan University, Changsha 410082, China^jAlso at Guangdong Provincial Key Laboratory of Nuclear Science, Institute of Quantum Matter, South China Normal University, Guangzhou 510006, China^kAlso at MOE Frontiers Science Center for Rare Isotopes, Lanzhou University, Lanzhou 730000, China^lAlso at Lanzhou Center for Theoretical Physics, Lanzhou University, Lanzhou 730000, China^mAlso at the Department of Mathematical Sciences, IBA, Karachi 75270, PakistanⁿAlso at Ecole Polytechnique Federale de Lausanne (EPFL), CH-1015 Lausanne, Switzerland^oAlso at Helmholtz Institute Mainz, Staudinger Weg 18, D-55099 Mainz, Germany

Abstract: By analyzing a $\psi(3686)$ data sample containing $(107.7 \pm 0.6) \times 10^6$ events taken with the BESIII detector at the BEPCII storage ring in 2009, the χ_{c0} resonance parameters are precisely measured using $\chi_{c0,c2} \rightarrow \pi^+\pi^-/K^+K^-$ events. The mass of χ_{c0} is determined to be $M(\chi_{c0}) = (3415.63 \pm 0.07 \pm 0.07 \pm 0.07) \text{ MeV}/c^2$, and its full width is $\Gamma(\chi_{c0}) = (12.52 \pm 0.12 \pm 0.13) \text{ MeV}$, where the first uncertainty is statistical, the second systematic, and the third for mass comes from χ_{c2} mass uncertainty. These measurements improve the precision of χ_{c0} mass by a factor of four and width by one order of magnitude over the previous individual measurements, and significantly boost our knowledge about the charmonium spectrum. Together with additional $(345.4 \pm 2.6) \times 10^6$ $\psi(3686)$ data events taken in 2012, the decay branching fractions of $\chi_{c0,c2} \rightarrow \pi^+\pi^-/K^+K^-$ are measured as well, with precision improved by a factor of three compared to previous measurements. These χ_{c0} decay branching fractions provide important inputs for the study of glueballs.

Keywords: χ_{c0} , BESIII, charmonium, resonance parameter, branching fraction

DOI: 10.1088/1674-1137/ade95f **CSTR:** 32044.14.ChinesePhysicsC.49091001

Charmonium, the bound state of charm and anti-charm quarks governed by the strong force, is analogous to the ‘hydrogen atom’ in the study of meson spectro-

scopy [1, 2]. Due to its heavy mass, the velocity of the charm quark is relative slow and therefore the system can be well described by a non-relativistic potential model

[3]. By now, the charmonium spectroscopy below the open-charm threshold is well established [4], and a precise study of them is important and necessary for a stringent test of the theory of the strong interaction, quantum chromodynamics (QCD). The χ_{cJ} (spin $J=0,1,2$) charmonia are P -wave $c\bar{c}$ states split by spin-orbit and tensor forces. At the moment, the χ_{c1} and χ_{c2} masses are precisely measured using a scan approach with $p\bar{p}$ annihilation by the E760 [5] and E835 [6] experiments, and by the LHCb [7] experiment in pp collisions, whereas a precise χ_{c0} mass measurement is relatively marginal, with an uncertainty about five times larger [8, 9] than that of $\chi_{c1,c2}$. Improved precision on the χ_{c0} mass is important for probing the spin structure of the strong force, such as the fine structure splitting $M(^3P_2) - M(^3P_0)$, and the singlet-triplet splitting $M(^1P_1) - M_{\text{cog}}(^3P_J)$, where $M_{\text{cog}}(^3P_J)$ is the center-of-gravity of the triplet. This helps precisely determine the spin-orbit and tensor forces.

We also lack knowledge about the precise width of χ_{c0} [4] compared to its $J=1, 2$ partners [5–7]. A precise width measurement of χ_{c0} serves as an essential input for studying the χ_{c0} decay, such as the $E1$ transition partial width, light hadron decay width, etc. Furthermore, lattice QCD calculations show an excited scalar glueball candidate with mass in the range of 2.8–3.7 GeV [10–13], and the χ_{c0} might contain a gluonic admixture due to the presence of such a nearby glueball. In this sense, the precise χ_{c0} width provides valuable knowledge to investigate the excited glueball spectrum, which was used to explain the $\gamma^* \rightarrow (c\bar{c})(c\bar{c})$ cross section discrepancy [14] between perturbative QCD calculations [15, 16] and the experimental measurement [17].

The decay of χ_{c0} to light hadrons proceeds predominantly via two-gluon exchanges (color-singlet) [18]. The decay widths of the simplest pseudo-scalar final state $\pi^+\pi^-$ and K^+K^- are expected to be identical within SU(3) flavor symmetry. This simple feature also applies to other 0^{++} systems, such as the light glueball candidates $f_0(1500)$ and $f_0(1710)$ [4]. However, the couplings of $f_0(1710)$ to the $\pi^+\pi^-$ and K^+K^- final states differ significantly [19, 20] due to a so-called 'Chiral Suppression' effect [21, 22]. Therefore, a precise measurement of the branching fraction (BF) $\chi_{c0} \rightarrow \pi^+\pi^-/K^+K^-$, together with its full width, provides an ideal testing ground for the study of decays of the glueball candidates. In addition, the color-octet component also plays an important role in charmonium decays, and these precise BF measurements can help to constrain the non-perturbative parameters in QCD calculations [18, 23, 24] and to allow us to finally understand the decay dynamics of charmonium states.

In this Letter, a precise mass and width measurement of χ_{c0} is achieved via $\chi_{c0} \rightarrow \pi^+\pi^-/K^+K^-$ decays. The decay BFs of $\chi_{c0,c2} \rightarrow \pi^+\pi^-/K^+K^-$ are precisely measured as well. The analysis is performed using a $\psi(3686)$ data sample consisting of $(107.7 \pm 0.6) \times 10^6$ events taken in

2009 and $(345.4 \pm 2.6) \times 10^6$ events taken in 2012 [25] at BESIII. The $\chi_{c0,c2}$ states are produced copiously in the radiative transition $\psi(3686) \rightarrow \gamma\chi_{c0,c2}$.

The BESIII detector is described in detail elsewhere [26]. Simulated Monte Carlo (MC) samples produced with a GEANT4-based [27] MC simulation software package, which includes the geometric description of the detector as well as its response, are used to determine detection efficiencies, optimize the selection criteria, and estimate background contributions. Signal MC samples of $\psi(3686) \rightarrow \gamma\chi_{c0,c2} \rightarrow \gamma\pi^+\pi^-/\gamma K^+K^-$ are produced. Each channel contains 400,000 signal events. In the simulation, the $\psi(3686)$ resonance is generated with KKMC [28, 29], which includes initial-state-radiation and the beam energy spread. The decays of $\psi(3686) \rightarrow \gamma\chi_{c0,c2} \rightarrow \gamma\pi^+\pi^-/\gamma K^+K^-$ are simulated with the angular distribution taken into account using a previous multipole amplitude measurement by BESIII [30].

To investigate the potential background, an inclusive MC sample containing the same number of $\psi(3686)$ events as data is simulated. This sample includes the production of the $\psi(3686)$ resonance, the ISR production of the J/ψ , and the continuum processes incorporated in KKMC [28, 29]. All particle decays are modeled with EVTGEN [31, 32] using BFs either taken from the Particle Data Group (PDG) [4], when available, or otherwise modeled with LUNDCHARM [33, 34] for all remaining unknown charmonium decays. Final state radiation (FSR) from charged final state particles is incorporated using the PHOTOS package [35]. Di-muon and Bhabha MC samples, each containing one million events, are generated with the Babayaga generator [36] for further background studies.

For the $\psi(3686) \rightarrow \gamma\chi_{c0,c2} \rightarrow \gamma\pi^+\pi^-/\gamma K^+K^-$ signal events of interest, the final states have two high-momentum charged tracks and an energetic radiative photon, with an energy of 261 (128) MeV in the χ_{c0} (χ_{c2}) case, due to the large mass gap between $\psi(3686)$ and $\chi_{c0,c2}$. Charged tracks detected in the multi-layer drift chamber (MDC) are required to be within the polar angle range $|\cos\theta| < 0.93$, where θ is defined with respect to the z axis, which is the symmetry axis of the MDC. For each good charged track, the distance of closest approach to the interaction point (IP) must be less than 10 cm along the z axis, and less than 1 cm in the transverse plane. A candidate event is required to have two good charged tracks with zero net charge.

Photon candidates are identified using isolated showers in the electromagnetic calorimeter (EMC). The deposited energy of each shower must be more than 25 MeV in the barrel region ($|\cos\theta| < 0.80$) and more than 50 MeV in the end-cap region ($0.86 < |\cos\theta| < 0.92$). To exclude showers that originate from charged tracks, the angle subtended by the EMC shower and the position of the closest charged track at the EMC must be greater than

10 degrees as measured from the IP. To suppress electronic noise and showers unrelated to the event, the difference between the EMC time and the event start time is required to be within $[0, 700]$ ns. At least one good photon candidate is required in an event.

To improve the momentum resolution of final state particles and further suppress background, a four-constraint (4C) kinematic fit which constrains the four-momentum of two charged tracks and a photon to the initial $\psi(3686)$ four-momentum is performed. The two charged tracks are assumed to be either $\pi^+\pi^-$ or K^+K^- , and the corresponding kinematic fit chi-squares ($\chi_{\gamma\pi^+\pi^-}^2$ and $\chi_{\gamma K^+K^-}^2$) are obtained. An event is assigned as $\gamma\pi^+\pi^-$ if $\chi_{\gamma\pi^+\pi^-}^2 < \chi_{\gamma K^+K^-}^2$, otherwise as γK^+K^- . The radiative photon candidate is selected as the one that yields the smallest χ^2 from the 4C kinematic fit if there are multiple photon candidates within one event. The χ^2 of the kinematic fit is further required to be less than 60 for $\gamma\pi^+\pi^-$ events and 56 for γK^+K^- events, which are optimized by maximizing the Figure-of-Merit $S/\sqrt{S+B}$, where S represents the number of normalized events from signal MC samples according to BFs from the PDG [4], and B is the total number of normalized background events estimated from the inclusive, Bhabha and di-muon MC samples.

For $\gamma\pi^+\pi^-$ events, there are radiative Bhabha and $\psi(3686) \rightarrow (\gamma)e^+e^-$ backgrounds. To remove these electrons, the deposited energy of each charged track in the EMC is required to be less than 1.34 GeV. Electrons passing through the EMC gap ($0.81 < |\cos\theta| < 0.86$), which has no crystals between the barrel and end-cap regions, can further survive. To remove these remaining electrons, the dE/dx of a charged particle measured by the MDC is used. For charged tracks falling into the gap region, the $|\chi_{dE/dx}(\pi)|$ [26] is required to be less than 2, where $\chi_{dE/dx}(\pi)$ is the pull value of dE/dx based on the pion hypothesis. The most significant background comes from radiative di-muon and $\psi(3686) \rightarrow (\gamma)\mu^+\mu^-$ events due to serious π and μ mis-identification. These non-peaking background processes are precisely known [4] and can be well simulated at BESIII.

For γK^+K^- events, the background level is much lower due to the higher kaon mass. There are some remaining backgrounds from radiative Bhabha, $\psi(3686) \rightarrow (\gamma)e^+e^-$, and $\psi(3686) \rightarrow \pi^0\pi^0 J/\psi \rightarrow \pi^0\pi^0 e^+e^-$, which are effectively vetoed by requiring the deposited energy of both kaons in the EMC to be less than 1.34 GeV. Since no particle identification is applied to high momentum pions and kaons, there is cross-contamination between $\gamma\pi^+\pi^-$ and γK^+K^- events. According to MC simulation studies, the cross-contamination ratio is small ($< 1\%$). For γK^+K^- events, the background contribution from $\gamma\pi^+\pi^-$ cross-contamination is fixed via MC simulation, and vice versa.

After applying the event selection criteria mentioned

above, the obtained $M(\pi^+\pi^-)$ and $M(K^+K^-)$ invariant mass distributions from data are shown in Fig. 1, where significant numbers of $\chi_{c0,c2}$ signal events are observed. To measure the mass and width of χ_{c0} , as well as the BFs of $\chi_{c0,c2} \rightarrow \pi^+\pi^-/K^+K^-$, an unbinned maximum likelihood fit is performed to the $\gamma\pi^+\pi^-$ and γK^+K^- data events simultaneously. In the fit, the BFs of $\chi_{c0,c2} \rightarrow \pi^+\pi^-$ and $\chi_{c0,c2} \rightarrow K^+K^-$ are shared as common parameters between data taken in different years. To avoid using the absolute momentum scale, and therefore significantly improve the mass precision of χ_{c0} , the mass split between χ_{c2} and χ_{c0} , $\Delta M_{20} \equiv M(\chi_{c2}) - M(\chi_{c0})$, is measured instead. Even in this case, the quality of the 2012 data is not as good as the 2009 data due to the worse MDC inner chamber performance during data taking [37], which bring in considerable systematic effects from discrepancies between data and MC simulation. Therefore, only the 2009 data are used for mass and width measurements, *i.e.* ΔM_{20} and the full width Γ of χ_{c0} are shared as common parameters in $\gamma\pi^+\pi^-$ and γK^+K^- data events taken in 2009.

The signal probability-density-function (PDF) is parameterized as

$$[\text{BW}^2(\sqrt{s}) \times \mathcal{P}S_1^2(\sqrt{s}) \times \mathcal{D}^2(\sqrt{s}) \times \mathcal{P}S_2^2(\chi_{c0,c2} \rightarrow \pi^+\pi^-/K^+K^-) \times \epsilon(\sqrt{s})] \otimes \text{Resolution}, \quad (1)$$

where $\text{BW}(\sqrt{s})$ is a relativistic Breit-Wigner (BW) amp-

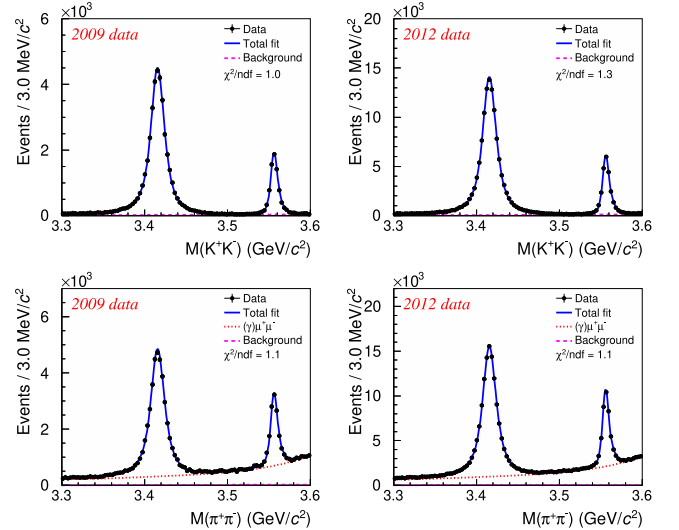


Fig. 1. (color online) The K^+K^- (top row) and $\pi^+\pi^-$ (bottom row) invariant mass distributions from $\psi(3686)$ data taken in 2009 (first column) and 2012 (second column) with fit results overlaid. The black dots with error bars are data, the blue solid curves represent the total fit results, the red dotted lines in bottom panels represent the background component from $(\gamma)\mu^+\mu^-$, and the pink dashed lines represent all other background components.

litude defined as

$$\text{BW}(\sqrt{s}) = \frac{1}{s - M^2 + iM\Gamma \frac{p}{p'} \frac{M}{\sqrt{s}}}, \quad (2)$$

where \sqrt{s} is the $\pi^+\pi^-/K^+K^-$ invariant mass, while M and Γ are the mass and constant width of $\chi_{c0,c2}$, respectively, and p (p') is the momentum of daughter particles in the rest frame of the mother particle with mass \sqrt{s} (M). In the $E1$ radiative transition $\psi(3686) \rightarrow \gamma\chi_{c0,c2}$, the decay width is proportional to a phase space factor $\mathcal{PS}_1(\sqrt{s})$ [38, 39] defined as

$$\mathcal{PS}_1(\sqrt{s}) = \left(\frac{E_\gamma}{E_\gamma^0} \right)^{3/2}, \quad (3)$$

where E_γ is the radiative photon energy and E_γ^0 corresponds to the photon energy at the $\chi_{c0,c2}$ mass M . An additional damping factor $\mathcal{D}(\sqrt{s}) = \left(\frac{(E_\gamma^0)^2}{E_\gamma^0 E_\gamma + (E_\gamma^0 - E_\gamma)^2} \right)^{1/2}$ [40] is also introduced to suppress the higher energy tail. $\mathcal{PS}_2(\chi_{c0,c2} \rightarrow \pi^+\pi^-/K^+K^-)$ is the phase space factor of $\chi_{c0,c2}$ decaying into $\pi^+\pi^-/K^+K^-$ [4]. The signal PDF is corrected by a mass-dependent efficiency curve $\epsilon(\sqrt{s})$, which is obtained by MC simulation studies and varies within 1% for the interested mass region, thus parameterized as a linear function. The $\chi_{c0,c2}$ resonance line shapes are further convolved with Gaussian functions to account for the detector resolution. In the fit, the χ_{c2} width is fixed to the known value [4], and the resolution difference between data and MC simulation measured from χ_{c2} data events is used to calibrate that for χ_{c0} .

The shapes of dominant background sources are described by polynomial functions. For γK^+K^- events, the background is low and parameterized as a free second-order polynomial. The small cross-contamination contribution from $\gamma\pi^+\pi^-$ events is fixed via MC simulation. For $\gamma\pi^+\pi^-$ events, the dominating $(\gamma)\mu^+\mu^-$ background is represented by a fourth-order polynomial, which is fixed according to normalized MC events for $\psi(3686) \rightarrow (\gamma)\mu^+\mu^-$ and di-muon processes. Other extra backgrounds with a small contribution ($\sim 3\%$ of the total background) are parameterized as a free second-order polynomial.

Figure 1 shows the fit results. The mass split between χ_{c2} and χ_{c0} is measured to be $\Delta M_{20} \equiv M(\chi_{c2}) - M(\chi_{c0}) = (140.54 \pm 0.07) \text{ MeV}/c^2$. Taking the world average mass $M(\chi_{c2}) = (3556.17 \pm 0.07) \text{ MeV}/c^2$ [4] as input, the χ_{c0} mass is calculated to be $M(\chi_{c0}) = (3415.63 \pm 0.07) \text{ MeV}/c^2$. The width of χ_{c0} is measured to be $\Gamma(\chi_{c0}) = (12.52 \pm 0.12) \text{ MeV}$. The uncertainties here are statistical only.

The systematic uncertainties in the mass split and χ_{c0} width measurements mainly come from the signal and

background PDF shapes as well as the damping factor, momentum-dependent scale, and possible interference effect. In the nominal fit model, a BW function with a mass-dependent width, *i.e.* Eq. (2), is used to describe the $\chi_{c0,c2}$ state. An alternative shape with a constant width BW function is investigated. The difference with respect to the nominal measurement for ΔM_{20} is $0.04 \text{ MeV}/c^2$ and for the χ_{c0} full width $\Gamma(\chi_{c0})$ is 0.08 MeV , which are taken as systematic uncertainties. A damping factor also appears in the signal PDF. We take another form $\mathcal{D}(\sqrt{s}) = e^{-E_\gamma^2/(8\beta^2)}$, where $\beta = 65.0 \pm 2.5 \text{ MeV}$ from the CLEO-c Collaboration [41]. The difference on the measurements of ΔM_{20} and $\Gamma(\chi_{c0})$ is $0.01 \text{ MeV}/c^2$ and 0.01 MeV , respectively.

The uncertainty due to background in the fit is studied in several aspects. The free background components are described by second-order polynomials for both $\gamma\pi^+\pi^-$ and γK^+K^- events. Changing this component to a third-order polynomial either for $\gamma\pi^+\pi^-$ or γK^+K^- events yields differences on the measurements, which are $0.02 \text{ MeV}/c^2$ for ΔM_{20} and 0.04 MeV for $\Gamma(\chi_{c0})$. Interference between $\chi_{c0,c2}$ resonances and continuum is observed in low-mass regions [42], and we account for this by adding the continuum component coherently to the signal PDF. The resulting difference for ΔM_{20} is $0.01 \text{ MeV}/c^2$ and $\Gamma(\chi_{c0})$ is 0.08 MeV . For $\gamma\pi^+\pi^-$ events, the dominant background comes from $(\gamma)\mu^+\mu^-$. Varying the output cross section from Babayaga [36] by $\pm 1\sigma$ for MC simulated background normalization yields a difference of $0.02 \text{ MeV}/c^2$ for ΔM_{20} and 0.02 MeV for $\Gamma(\chi_{c0})$. The shape parameters of this background component are also varied within $\pm 1\sigma$, which yields a difference of $0.01 \text{ MeV}/c^2$ for ΔM_{20} and 0.02 MeV for $\Gamma(\chi_{c0})$. The momentum-dependent scale is simulated by MC. The systematic uncertainty due to the difference between data and MC is studied by correcting the MC distribution of final-state particle momenta to data with χ_{c2} events, which yields a variation of $0.04 \text{ MeV}/c^2$ for ΔM_{20} and 0.01 MeV for $\Gamma(\chi_{c0})$.

Table 1 summarizes all these sources and their corresponding contributions. Assuming all the sources are independent, the total systematic uncertainty is obtained by adding each individual source in quadrature, which is $0.07 \text{ MeV}/c^2$ for ΔM_{20} and 0.13 MeV for $\Gamma(\chi_{c0})$.

The BF of $\chi_{c0,c2} \rightarrow \pi^+\pi^-/K^+K^-$ is calculated as

$$\mathcal{B} = \frac{N_{\text{sig}}}{N_{\text{tot}}[\psi(3686)]\epsilon\mathcal{B}[\psi(3686) \rightarrow \gamma\chi_{c0,c2}]}, \quad (4)$$

where N_{sig} is the number of observed $\chi_{c0,c2}$ signal events from the fit, $N_{\text{tot}}[\psi(3686)]$ is the total number of collected $\psi(3686)$ events [25], ϵ is the detection efficiency of $\gamma\pi^+\pi^-/\gamma K^+K^-$ events, and $\mathcal{B}[\psi(3686) \rightarrow \gamma\chi_{c0,c2}]$ is the BF of the $E1$ radiative transition [4]. In practice, a simultaneous fit is performed and the BFs are shared between dif-

Table 1. Sources of systematic uncertainties and their contributions to ΔM_{20} and $\Gamma(\chi_{c0})$ measurements.

Source	$\Delta M_{20} / (\text{MeV}/c^2)$	$\Gamma(\chi_{c0}) / \text{MeV}$
Signal shape	0.04	0.08
Damping factor	0.01	0.01
Polynomial background	0.02	0.04
Interference effect	0.01	0.08
Number of $(\gamma)\mu^+\mu^-$ background	0.02	0.02
Shape of $(\gamma)\mu^+\mu^-$ background	0.01	0.02
Momentum dependent scale	0.04	0.01
Total	0.07	0.13

ferent data sets. The BFs are measured to be $\mathcal{B}(\chi_{c0} \rightarrow K^+K^-) = (6.36 \pm 0.02) \times 10^{-3}$, $\mathcal{B}(\chi_{c0} \rightarrow \pi^+\pi^-) = (6.06 \pm 0.02) \times 10^{-3}$, $\mathcal{B}(\chi_{c2} \rightarrow K^+K^-) = (1.22 \pm 0.01) \times 10^{-3}$, and $\mathcal{B}(\chi_{c2} \rightarrow \pi^+\pi^-) = (1.61 \pm 0.01) \times 10^{-3}$, respectively, where all the uncertainties are statistical only. Table 2 lists the detection efficiencies for each data set.

The systematic uncertainties in the BF measurements mainly come from the total number of $\psi(3686)$ events, detection efficiencies, signal and background PDF shapes, possible interference effect, fit range, 4C kinematic fit, and intermediate BFs.

The total number of $\psi(3686)$ events is measured by counting inclusive hadronic events, with an uncertainty of 0.7% [25]. Detection efficiencies include tracking, photon detection, decay angular distributions, and selection criteria. The uncertainty of photon detection is measured to be 0.5% per photon by studying the $e^+e^- \rightarrow \gamma\mu^+\mu^-$ process and 0.5% is assigned for this analysis. Pion and kaon tracks have a momentum above 1 GeV. The tracking efficiency of such tracks is above 99% at BESIII, by studying $e^+e^- \rightarrow \pi^+\pi^-\pi^+\pi^-$ and $J/\psi \rightarrow K^*K$ events. According to the two-dimensional (2D, p_t vs. $\cos\theta$) tracking efficiencies of data and MC simulation, the uncertainty in each bin is obtained. The final uncertainty due to tracking is estimated as a weighted average over 2D bins.

Decay angular distributions also affect the detection efficiencies. Considering the helicity amplitudes and correlation coefficients measured by BESIII [30], 100 sets of two correlated helicity amplitude parameters are obtained via a 2D sampling. The resulting changes in detection efficiencies, and therefore the corresponding changes of BFs from the simultaneous fit, are taken as systematic uncertainties. The uncertainties due to the pion/kaon EMC deposit energy requirement and fit range are studied using a Barlow test [43], by changing a series of EMC deposit energies and fit ranges. All the alternative choices give results within 1σ of the nominal result, which means these two sources can be ignored.

For the 4C kinematic fit, a correction of the pull distribution of charged track parameters is applied to the MC

Table 2. The detection efficiencies for $\gamma\pi^+\pi^-$ and γK^+K^- data events taken in different years.

	$\epsilon(\gamma\pi^+\pi^-)$	$\epsilon(\gamma K^+K^-)$
2009 χ_{c0}	0.644 ± 0.001	0.589 ± 0.001
2009 χ_{c2}	0.667 ± 0.001	0.624 ± 0.001
2012 χ_{c0}	0.634 ± 0.001	0.577 ± 0.001
2012 χ_{c2}	0.658 ± 0.001	0.613 ± 0.001

Table 3. Sources of systematic uncertainties and their contributions (in %) to BF measurements. "... " means a non-applicable option.

Source	$\gamma\pi^+\pi^-$		γK^+K^-	
	χ_{c0}	χ_{c2}	χ_{c0}	χ_{c2}
$N_{\text{tot}}[\psi(2S)]$	0.7	0.7	0.7	0.7
Tracking	0.1	0.1	0.2	0.1
Photon	0.5	0.5	0.5	0.5
Polynomial background	0.6	0.2	0.1	0.1
Interference effect	0.4	0.0	0.4	0.0
Number of $(\gamma)\mu^+\mu^-$ background	0.1	0.4	0.1	0.1
Shape of $(\gamma)\mu^+\mu^-$ background	0.2	0.1	0.1	0.1
Cross contamination	0.0	0.0	0.0	0.1
Damping factor	0.1	0.2	0.1	0.1
Signal shape	0.1	0.2	0.1	0.1
Angular distribution	...	0.1	...	0.0
4C kinematic fit	0.3	0.2	0.7	0.8
Sum	1.2	1.1	1.2	1.2
Intermediate BF	2.1	2.1	2.1	2.1
Total	2.4	2.4	2.4	2.4

simulation [44]. The uncertainties are taken as half of the efficiency difference with or without helix parameter corrections. The uncertainties on the BFs for $\psi(3686) \rightarrow \gamma\chi_{c0}$ (2.1%) and $\psi(3686) \rightarrow \gamma\chi_{c2}$ (2.1%) are taken from the PDG [4]. The uncertainties due to the signal shape, damping factor and background are studied using the same method as the mass split and width measurement. The cross-contaminations between $\gamma\pi^+\pi^-$ and γK^+K^- events are studied via MC simulations, with input BFs updated by this measurement. The fluctuations due to BFs are taken as systematic uncertainties.

Table 3 summarizes all these sources and their contributions to the BF measurements. Assuming all the sources are independent, the total systematic uncertainties are obtained by adding them in quadrature. The largest systematic uncertainty comes from the intermediate BFs, and all other sources contribute about 1.2%.

In summary, a precise measurement of the χ_{c0} resonance parameters and the $\chi_{c0,c2} \rightarrow \pi^+\pi^-/K^+K^-$ decay BFs is

performed at BESIII by analyzing $\psi(3686)$ data events. The mass split between χ_{c2} and χ_{c0} is measured to be $\Delta M_{20} = (140.54 \pm 0.07 \pm 0.07) \text{ MeV}/c^2$. Taking the χ_{c2} world average mass as input, the χ_{c0} mass is determined to be $M(\chi_{c0}) = (3415.63 \pm 0.07 \pm 0.07 \pm 0.07) \text{ MeV}/c^2$, where the first uncertainty is statistical, the second systematic, and the third from the χ_{c2} mass uncertainty. This is the most precise χ_{c0} mass measurement to date. It is a bit higher ($1.42 \pm 0.49 \text{ MeV}/c^2$) than the BES measurement [8], while it agrees well with the E835 measurement [9]. Our measurement improves the precision of the χ_{c0} mass over previous individual measurements by a factor of four [8, 9]. The full width of χ_{c0} is measured to be $\Gamma(\chi_{c0}) = (12.52 \pm 0.12 \pm 0.13) \text{ MeV}$. It agrees with the BES measurement quite well within 1σ [8] and improves the precision by an order of magnitude. These measurements have a big impact on our knowledge about the χ_{c0} resonance parameters [4], and are expected to play a crucial role in our understanding of the strong force governing the $c\bar{c}$ system [39, 45]. A comparison of our results with other measurements as well as the PDG world average is shown in Fig. 2.

The decay BF's are measured to be

$$\begin{aligned}\mathcal{B}(\chi_{c0} \rightarrow K^+ K^-) &= (6.36 \pm 0.02 \pm 0.08 \pm 0.13) \times 10^{-3}, \\ \mathcal{B}(\chi_{c0} \rightarrow \pi^+ \pi^-) &= (6.06 \pm 0.02 \pm 0.07 \pm 0.13) \times 10^{-3}, \\ \mathcal{B}(\chi_{c2} \rightarrow K^+ K^-) &= (1.22 \pm 0.01 \pm 0.02 \pm 0.03) \times 10^{-3}, \\ \mathcal{B}(\chi_{c2} \rightarrow \pi^+ \pi^-) &= (1.61 \pm 0.01 \pm 0.02 \pm 0.04) \times 10^{-3},\end{aligned}$$

where the first uncertainties are statistical, the second systematic, and the third come from $\mathcal{B}[\psi(3686) \rightarrow \gamma\chi_{c0,c2}]$ [4]. These measurements agree with the CLEO-c result within 1σ [46], and improve the precision by more than threefold. Interestingly, the ratio of BF's $\mathcal{R} = \frac{\mathcal{B}(\chi_{c0} \rightarrow \pi^+ \pi^-)}{\mathcal{B}(\chi_{c0} \rightarrow K^+ K^-)} = (0.95 \pm 0.01 \pm 0.01)$ demonstrates no obvious ‘Chiral Suppression’ is observed for this 0^{++} system, which supports the theoretical analysis in Ref.

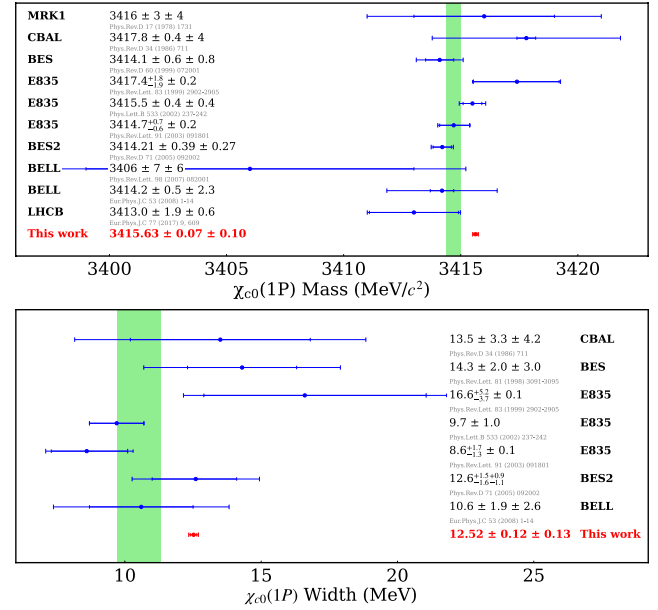


Fig. 2. (color online) Comparison of the χ_{c0} resonance parameters measurements. The light green bands represent the PDG world average [4].

[47, 48]. This behavior is also quite different from the case of the $f_0(1710)$ [19, 20], therefore challenging the scalar glueball interpretation of the $f_0(1710)$ state [21]. It implies $f_0(1710)$ might contain a substantial $s\bar{s}$ component, which aligns with the model calculations in Ref. [49, 50]. Combining our precisely measured \mathcal{R} value, which constrains the glueball fraction in $f_0(1710)$, with future theoretical improvements will advance our understanding of QCD.

ACKNOWLEDGEMENTS

The BESIII Collaboration thanks the staff of BEPCII and the IHEP computing center for their strong support. We are also grateful to Prof. Chen Ying for the inspiring discussion on glueballs.

References

- [1] T. Appelquist, A. De Rújula, H. D. Politzer *et al.*, *Phys. Rev. Lett.* **34**, 365 (1975)
- [2] E. Eichten, K. Gottfried, T. Kinoshita *et al.*, *Phys. Rev. Lett.* **34**, 369 (1975) [Erratum: *Phys. Rev. Lett.* **36**, 1276 (1976)]
- [3] E. Eichten, K. Gottfried, T. Kinoshita *et al.*, *Phys. Rev. D* **17**, 3090 (1978)
- [4] S. Navas *et al.* (Particle Data Group), *Phys. Rev. D* **110**, 030001 (2024)
- [5] T. A. Armstrong *et al.* (E760), *Nucl. Phys. B* **373**, 35 (1992)
- [6] M. Andreotti *et al.*, *Nucl. Phys. B* **717**, 34 (2005), arXiv: hepex/0503022
- [7] R. Aaij *et al.* (LHCb), *Phys. Rev. Lett.* **119**, 221801 (2017), arXiv: 1709.04247[hep-ex]
- [8] M. Ablikim *et al.* (BES), *Phys. Rev. D* **71**, 092002 (2005), arXiv: hep-ex/0502031
- [9] S. Bagnasco *et al.* (Fermilab E835), *Phys. Lett. B* **533**, 237 (2002)
- [10] C. J. Morningstar and M. J. Peardon, *Phys. Rev. D* **60**, 034509 (1999), arXiv: hep-lat/9901004
- [11] E. Gregory, A. Irving, B. Lucini *et al.*, *JHEP* **10**, 170 (2012), arXiv: 1208.1858[hep-lat]
- [12] H. B. Meyer, *Glueball regge trajectories*, Other thesis (2004), arXiv: hep-lat/0508002
- [13] Y. Chen *et al.*, *Phys. Rev. D* **73**, 014516 (2006), arXiv: hep-lat/0510074
- [14] S. J. Brodsky, A. S. Goldhaber, and J. Lee, *Phys. Rev. Lett.* **91**, 112001 (2003), arXiv: hep-ph/0305269
- [15] E. Braaten and J. Lee, *Phys. Rev. D* **67**, 054007 (2003)

- [Erratum: *Phys. Rev. D* **72**, 099901 (2005)], arXiv: [hep-ph/0211085](#)
- [16] K. Y. Liu, Z. G. He, and K. T. Chao, *Phys. Lett. B* **557**, 45 (2003), arXiv: [hep-ph/0211181](#)
- [17] K. Abe *et al.* (Belle), *Phys. Rev. Lett.* **89**, 142001 (2002), arXiv: [hep-ex/0205104](#)
- [18] H. W. Huang and K. T. Chao, *Phys. Rev. D* **54**, 6850 (1996) [Erratum: *Phys. Rev. D* **56**, 1821 (1997)], arXiv: [hep-ph/9606220](#)
- [19] M. Ablikim *et al.* (BES), *Phys. Lett. B* **603**, 138 (2004), arXiv: [hep-ex/0409007](#)
- [20] M. Ablikim *et al.*, *Phys. Lett. B* **642**, 441 (2006), arXiv: [hep-ex/0603048](#)
- [21] M. Chanowitz, *Phys. Rev. Lett.* **95**, 172001 (2005), arXiv: [hep-ph/0506125](#)
- [22] K. T. Chao, X. G. He, and J. P. Ma, *Phys. Rev. Lett.* **98**, 149103 (2007), arXiv: [0704.1061\[hep-ph\]](#)
- [23] G. T. Bodwin, E. Braaten, and G. P. Lepage, *Phys. Rev. D* **46**, R1914 (1992), arXiv: [hep-lat/9205006](#)
- [24] J. Bolz, P. Kroll, and G. A. Schuler, *Phys. Lett. B* **392**, 198 (1997), arXiv: [hep-ph/9610265](#)
- [25] M. Ablikim *et al.* (BESIII), *Chin. Phys. C* **48**, 093001 (2024), arXiv: [2403.06766\[hep-ex\]](#)
- [26] M. Ablikim *et al.* (BESIII), *Nucl. Instrum. Meth. A* **614**, 345 (2010), arXiv: [0911.4960\[physics.ins-det\]](#)
- [27] S. Agostinelli *et al.* (GEANT4), *Nucl. Instrum. Meth. A* **506**, 250 (2003)
- [28] S. Jadach, B. F. L. Ward, and Z. Was, *Phys. Rev. D* **63**, 113009 (2001)
- [29] S. Jadach, B. Ward, and Z. Was, *Computer Physics Communications* **130**, 260325 (2000)
- [30] M. Ablikim *et al.* (BESIII), *Phys. Rev. D* **84**, 092006 (2011), arXiv: [1110.1742\[hep-ex\]](#)
- [31] D. J. Lange, *Nucl. Instrum. Meth. A* **462**, 152 (2001)
- [32] R. G. Ping, *Chin. Phys. C* **32**, 599 (2008)
- [33] J. C. Chen, G. S. Huang, X. R. Qi *et al.*, *Phys. Rev. D* **62**, 034003 (2000)
- [34] R. L. Yang, R. G. Ping, and H. Chen, *Chin. Phys. Lett.* **31**, 061301 (2014)
- [35] E. Barberio, B. van Eijk, and Z. Was, *Computer Physics Communications* **66**, 115 (1991)
- [36] G. Balossini, C. Bignamini, C. M. C. Calame *et al.*, *Phys. Lett. B* **663**, 209 (2008), arXiv: [0801.3360\[hep-ph\]](#)
- [37] M. Ablikim *et al.* (BESIII), *Chin. Phys. C* **42**, 023001 (2018), arXiv: [1709.03653\[hep-ex\]](#)
- [38] N. Brambilla *et al.*, *Eur. Phys. J. C* **71**, 1534 (2011), arXiv: [1010.5827\[hep-ph\]](#)
- [39] T. Barnes, S. Godfrey, and E. S. Swanson, *Phys. Rev. D* **72**, 054026 (2005), arXiv: [hep-ph/0505002](#)
- [40] V. V. Anashin *et al.*, *Int. J. Mod. Phys. Conf. Ser.* **02**, 188 (2011), arXiv: [1012.1694\[hep-ex\]](#)
- [41] R. E. Mitchell *et al.* (CLEO), *Phys. Rev. Lett.* **102**, 011801 (2009) [Erratum: *Phys. Rev. Lett.* **106**, 159903 (2011)], arXiv: [0805.0252\[hep-ex\]](#)
- [42] S. Dobbs, A. Tomaradze, T. Xiao *et al.*, *Phys. Rev. D* **91**, 052006 (2015), arXiv: [1502.01686\[hep-ex\]](#)
- [43] R. Barlow, in *PHYSTAT (2005): Statistical Problems in Particle Physics, Astrophysics and Cosmology*, (2004) pp. 56–59, arXiv: [physics/0406120](#)
- [44] M. Ablikim *et al.* (BESIII), *Phys. Rev. D* **87**, 012002 (2013), arXiv: [1208.4805\[hep-ex\]](#)
- [45] W. Lucha, F. F. Schoberl, and D. Gromes, *Phys. Rept.* **200**, 127 (1991)
- [46] D. M. Asner *et al.* (CLEO), *Phys. Rev. D* **79**, 072007 (2009), arXiv: [0811.0586\[hep-ex\]](#)
- [47] K. T. Chao, X. G. He, and J. P. Ma, *Eur. Phys. J. C* **55**, 417 (2008), arXiv: [hep-ph/0512327](#)
- [48] Z. F. Zhang and H. Y. Jin, (2005), arXiv: [hep-ph/0511252](#)
- [49] F. E. Close and Q. Zhao, *Phys. Rev. D* **71**, 094022 (2005), arXiv: [hep-ph/0504043](#)
- [50] S. Narison, *Phys. Rev. D* **73**, 114024 (2006), arXiv: [hep-ph/0512256](#)